Symposium on Applied Aerodynamics and Design of Aerospace Vehicle (SAROD 2011)
November 16-18, 2011, Bangalore, India

REYNOLDS NUMBER AND LEADING EDGE BLUNTNESS EFFECTS ON 65° DELTA WING AT SUBSONIC SPEED

Anand R Rao*, Buddhadeb Nath*, Gopinath.N* and Krishna Rakend Reddy. D+
National Aerospace Laboratories, Bangalore, India

ABSTRACT

The vortex properties over a delta wing depend mainly on angle of attack (α), Mach number (M), Reynolds number (R_e) and leading edge (LE) bluntness. In the case of delta wing with blunt LE, separation of the primary vortex is from the tip of the wing .To study the effect of LE bluntness and Reynolds number experiments were carried out on delta wings with 65° sweep. Four models with different wing leading edge (LE) radii were tested in wind tunnel. The experiments were carried out in the Mach number range of 0.3 to 1.2 in the 1.2m Trisonic wind tunnel at NAL. Angle of attack was varied from -5° to 26°. The forces and moments were measured using six components balance. Studies were also conducted to obtain Surface flow visualization using oil flow technique. Surface flow visualization data has been used to correlate force measurement data. Results show that flow at higher Reynolds number exhibits higher lift. The higher Reynolds number flow displays severe pitch up compared to low Reynolds number flow. Lift and pitching moment characteristics are strong function of Leading edge bluntness. With increase in LE bluntness overall lift decreases.

Key Words: Vortex breakdown, Leading edge bluntness, Reynolds number

NOMENCLATURE

α	Angle of attack (deg)
M	Free stream Mach number
R_e	Reynolds Number
R_{le}	Leading Edge Radius (mm)
Cl	Coefficient of lift
Cpm	Coefficient of Pitching moment
P_0	Tunnel stagnation pressure

1. INTRODUCTION

Delta wing has been a subject of intense research since decades due to its inherent characteristics of generating increased nonlinear lift due to vortex dominated flows. Lot of work has been carried out in order to understand vortex dominated flows on 65° delta wing [6, 7]. Pitch up is a major concern in delta wing type aircrafts. Pitch up is due to breakdown of primary vortex at the trailing edge of the wing. In tailless wings pitch up leads to severe stability problems. One of factors which affect vortex breakdown is leading edge bluntness. Unlike sharp leading edge delta wings, flow over delta wings with leading edge radius is a strong function of Reynolds number. In general vortex properties over a Delta wing depend mainly on angle of attack (α), Mach Number (M), Reynolds number (R_e) and leading edge (LE) bluntness. In the case of delta wing with blunt LE, the primary separation is no longer initiated at the apex of leading edge and origin of the vortex separation is from the tip of the wing [1,2]. To study the effect of LE bluntness and Reynolds number experiments were carried out on delta wings with 65° sweep. Four different wings with leading edge (LE) radii, sharp (R_{le}=0mm), small (R_{le}=0.625mm), medium (R_{le}=1.25mm) and large (R_{le}=2.5mm) fig (1, 2) were tested in wind tunnel. The experiments were carried out in the Mach number range of 0.3 to 1.2 in the 1.2m Trisonic wind tunnel at NAL. Angle of attack was varied from -5° to 26°. The forces and moments were measured using six components balance on four delta wing models. Surface oil flow visualization studies were also conducted. The paper presents results and analysis on the effect of Reynolds number and Leading Edge bluntness at subsonic speeds.

2. EXPERIMENTAL DETAILS

2.1 Facility

The wind tunnel is an intermittent blow down type with a square test section 1.2m x1.2m and capable of generating controlled flow at subsonic, transonic and supersonic speeds (Mach number 0.2 to 4.0). Supersonic speeds are achieved by variation of nozzle contour through a flexible nozzle, transonic Mach numbers are tested using a transonic insert, which features a perforated wall test section. The top and bottom walls of the insert have 0.5″ diameter 60° inclined holes with 6% open area ratio; the sidewalls have normal holes with an open area ratio of 20%.

*Scientists, NTAF Division, NAL, Bangalore

+Project Trainee, NTAF Divsn, NAL, Bangalore

Model incidence can be varied in the incidence range of –15° to 26° in the step and pause, continuous and Pre-position modes [5]. The three forces and moments were measured by six components 1.50" ABLE MK XXI L balance. Tunnel static and total pressures were measured by using ± 15 psi differential transducers. Increase in Reynolds number is achieved by increasing blowing pressure or Tunnel stagnation pressure (P_0).

2.2 Model

Four dedicated metallic models were fabricated. All the models had a sweepback angle of 65 deg, maximum root chord of 375mm and maximum span of 349mm, as shown in Figure 1. Distinguishing feature being Leading Edge Radius (R_{le}) of sharp (R_{le}=0mm), small (R_{le}=0.625mm), medium (R_{le}=1.25mm) and large (R_{le}=2.5mm) as shown in Figure 2 Top surfaces of all the models were kept flat. Bottom surfaces were provided with a metric cylindrical attachment to suit 1.50" ABLE MK XXI L balance. Reference area of the wing is 101.64 sq. in. Boundary layer trip was applied on the top and bottom surfaces of the wing in order to simulate the turbulent boundary layer over major portion of the model. The surface of the model was painted black in color to ensure the proper and distinct visibility of stream line patterns. A mixture of titanium dioxide, oleic acid & silicone oil in the volumetric ratio of 10:5:1 has been used for surface flow visualisation studies.

3. DISCUSSION OF TEST RESULTS

3.1 Force Measurements

3.1.1 Effect of Reynolds Number

Experiments were conducted at two distinct Reynolds numbers (R_e) of 2.7 million and 5.4 million at Mach no 0.3. Effect of Reynolds number at M=0.3 for different LE radii, (R_{le}=0.0 to 2.5mm) is presented with results. Reynolds number has been calculated based on mean aerodynamic chord. For delta wing with leading edge radius, R_{le}= 0.0mm higher Reynolds number flow shows higher lift throughout the range of incidence 0° to 25° compared to flow with lower Reynolds number Figure 3 . The drop in lift (kink) occurs around angle of attack of 17° for higher R_e which is due to vortex breakdown [2]. Whereas for lower R_e , the kink in the lift curve is not prominent. In Delta wing with leading edge radius, R_{le}=0.625mm, the difference in lift between the two lift curves due the Reynolds number (effect) narrows down Figure 4. The kink in the lift curve occurs around angle of attack of 17° for both Reynolds numbers curves. For wing with the leading edge radius R_{le}=1.25mm difference in lift values between flow with R_e = 2.7 and 5.4 million is negligible Figure 5. The drop in lift occurs around angle of attack of 14° for both the cases. When leading edge radius is increased to R_{le}=2.5mm difference in lift due to Reynolds number is significant Figure 6. Flow at higher Reynolds number shows higher lift in the angle of attack range 2.5° to 17°. Drop in the lift occurs on this curve around α =17°. For flow with R_e = 2.7 million the kink in lift curve occurs later around α =22.5°. For delta wing with leading edge radius, R_{le} = 0.0 and 2.5 mm, higher Reynolds number flow shows higher lift throughout the range of incidence 0° to 25° compared to lower Reynolds number. Whereas for intermediate thickness R_{le} = 0.625 mm and 1.25 mm, effect of Reynolds number is insignificant. It is of interest to note that this drop in the lift depends strongly on leading edge radius for a given Reynolds number. Also the flow at the higher Reynolds number exhibits sharper drop in the lift curve as compared to low R_e flow indicating intensity of vortex breakdown is different for different leading radii.

For leading edge with R_{le} = 0.0mm pitching moment characteristic Figure 7 shows that the magnitude of pitching moment generated for flow with R_e = 5.4million is higher and the pitch up occurs around α =15° and pitch up slope is sharper for higher R_e flow than for low R_e flow. The wing with R_{le}=0.625mm exhibits slightly higher pitching moment values for flow with R_e =5.4 million and pitch up occurs around α = 14°, the angle around which drop in the lift curve occurs for both the Reynolds numbers Figure 8. The slope or severity of pitch up is almost same for both the cases. In case of wing with the leading edge radius, R_{le}=1.25mm magnitude of pitching moment values are almost same for the two Reynolds numbers Figure 9. The pitch up first occurs for flow at R_e =2.7 million around α = 14° corresponding to kink in lift curve and for flow at R_e = 5.4 million, pitch up is seen around 15°. Slopes of the pitch up are almost same. Finally for wing with leading edge radius, R_{le}=2.5mm, the magnitude of pitching moment for R_e = 5.4 million case is higher as compared to flow with R_e = 2.7 million Figure 10. Pitch up occurs around α =15° for R_e = 5.4 million. However, for flow with R_e = 2.7 million pitch up occurs later around α =22.5° where the kink in lift curve is seen. Both these curves have sharp pitch up. The magnitude of pitching moment does not vary much with Reynolds number. But, angle at which pitch up occurs and sharpness of pitch up curve depend on the Reynolds number.

3.1.2 Effect of Leading Edge Bluntness

Effect of LE bluntness is shown at M=0.3 for R_e = 2.7 million and M=0.4 at R_e=3.4 million, Figure 11. At these two Mach numbers, lift curves show that with increase in LE bluntness overall lift value decreases. At both Mach numbers in the range of incidence α =-5° to 5°, the lift coefficient does not vary much with change in the bluntness. Subsequently in the incidence range of α = 5° to 18°, effect of bluntness is seen on the lift. At M=0.3 for leading edge radii R_{le}=0.0 and 0.625 mm, overall lift values are almost same in both the cases. There is drop in the lift with increasing radius. For wing with leading edge radius, R_{le}=1.25mm the lift values are positioned between lift curves for R_{le}=0.0 mm, 0.625mm and Rle=2.5mm in the incidence range 10° to 16°. The kink in lift curve for radii R_{le}=0.0, 0.625 and 1.25mm occurs around α= 14° and for R_{le}=2.5mm, the kink appears around α=22.5°.

At Mach number 0.4, increase in the nonlinear lift slope is rapid for the wing with leading edge radius, R_{le}=0.0mm Figure 12. The lift curve slopes gradually decrease with increasing bluntness. This is due to different rates of separation and subsequent vortex formation on the delta wings. Beyond angle of attack of 18° (subsequent to vortex breakdown) there is no variation in lift with bluntness for first three radii (R_{le}=0, 0.625, 1.25mm) but for the large radius, R_{le}=2.5mm there is decrease in lift. A kink is observed around α=14° for R_{le}=0mm, R_{le}=0.625mm and R_{le}=1.25mm cases, whereas the appearance of kink is delayed to around α=22.5° for R_{le}=2.5mm case due to vortex breakdown. At both Mach numbers, similarity in pitching moment characteristics is exhibited, Figure 13 and Figure 14 for all the leading edge radii, R_{le}=0.0, 0.625, 1.25 and 2.5 mm. Pitch up occurs around α =14°(M =0.3 and 0.4) for R_{le} = 0.0mm and for R_{le}=2.5mm, pitching moment curve shows it around α=22.5°(M = 0.3) and 21°(M=0.4). Pitch up becomes sharper as LE bluntness increases. The leading edge radii R_{le}=0.0 and 0.625mm show highly stable characteristics in the angle of attack range of 2° to 14°. Whereas the leading edge radii, R_{le}=1.25 and 2.5mm show neutrally stable characteristics up to α=10°, subsequently beyond this angle of attack it changes to highly stable characteristics till pitch up.

3.2 Surface Flow Visualisation

The surface oil flow visualisation data is correlated with force data. Surface oil flow pictures show a comparative surface flows for two leading edge radii R_{le}=0mm and R_{le}=2.5mm at M = 0.4 and at angle of attack α=15°. For leading edge radius R_{le}=0mm at α=15°, around initiation of pitch up, surface oil flow clearly indicates well developed LE vortices, primary attachment line, secondary separation line and centrally attached flow as shown in Figure 15 and Figure 17 . Correlating this data with the corresponding force data it is seen for R_{le}=0.0mm, around this incidence a kink in lift curve and correspondingly pitch up (initiation) in the pitching moment curve is observed. The vortex breakdown initially takes place in core of vortex. Oil flow does not show traces of vortex break down Whereas for R_{le}=2.5mm and α=15°, Figure 16 shows not so well formed attachment line for primary vortex over the wing surface. The lift curve does not show any kink correspondingly no pitch up (initiation) in the pitching moment curve at this incidence. Separation of the flow from the leading edge and subsequent formation of the vortex is at different stages depending on the LE bluntness and the impact of this flow structure can be seen clearly on the non linear lift slopes around α =15°[3,4].

4. CONCLUSION

Experiments were conducted on 65° delta wing to study the effect of Reynolds number and varying leading edge radius. Following are the conclusions:

(1) For delta wing with leading edge $R_{le=}$ 0.0 mm and 2.5 mm higher Reynolds number flow R_e =5.4 million shows higher lift throughout the range of incidence 0° to 25° compared to flow with R_e=2.7million .Whereas for intermediate thickness, R_{le} = 0.625 and 1.25 mm insignificant effect on lift is seen in this range of Reynolds number. The flow at the higher Reynolds number exhibits sharper drop in the lift curve as compared to low R_e flow indicating intensity of vortex breakdown is different for different leading edge radii.

(2) The magnitude of pitching moment does not vary much with Reynolds number. But angle at which pitch up occurs and severity of pitch up depends on the Reynolds number.

(3) The lift and pitching moment characteristics are strong function of Leading edge bluntness. With increase in LE bluntness overall lift decreases. In case of large LE bluntness, pitch up occurs at later stage (α=22.5°) as compared to sharp LE (α=14°). Slope of pitch up becomes sharper and severe as LE bluntness increases.

(4) The surface oil flow visualisation studies conducted at M=0.4; α=14° on two leading edge radii, R_{le}=0.0mm and R_{le}=2.5mm show different flow structure indicating variation of flow structure with LE bluntness.

Acknowledgment

The authors acknowledge with thanks to (1) Dr. K.Y. Narayan and Dr. S.N. Seshadri for providing the experimental data (2) Director, NAL and Head, NTAF for providing an opportunity to work on Delta wings through In-house sponsored project (3) Mr.Babu Rajan for the photography.

REFERENCES

1. Luckring J M, "Compressibility and leading-edge bluntness effects on a 65° delta wing", AIAA Paper 2004-765, January 2004.
2. Earnshaw P B, Lawford J A. "Low speed wind tunnel experiments on a series of sharp-edged delta Wings", ARC Reports and Memoranda No.3424, March 1964.
3. K. Y. Narayan, Seshadri S N. "Vortical flows on lee surface of delta wings", NAL TM AE 8802, June 1988.
4. Gopinath N. "Experiments on 60° swept delta wing-body with flaps", NAL PD NT 0407, June 2004.
5. Anon…….: "4 ft Trisonic wind tunnel Users' Manual", January 1973.
6. K. Y. Narayan, K. Hartmann. "Transonic and Supersonic Flow Past a 65 deg Delta Wing with Rounded Leading Edges – Analysis of Experimental Data", NAL TM AE 8806, December 1988.
7. N.C. Lambourne and D.W. Bryer. "Some Measurements in the Vortex Flow Generated by a Sharp Leading Edge having 65 degrees Sweep", C.P. No. 477, A.R.C. Technical Report, 1960.

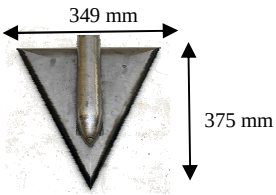

Figure 1. Wing configuration

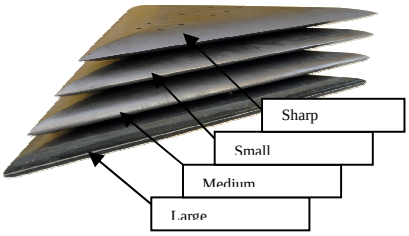

Figure 2. Wings with different leading edge radii

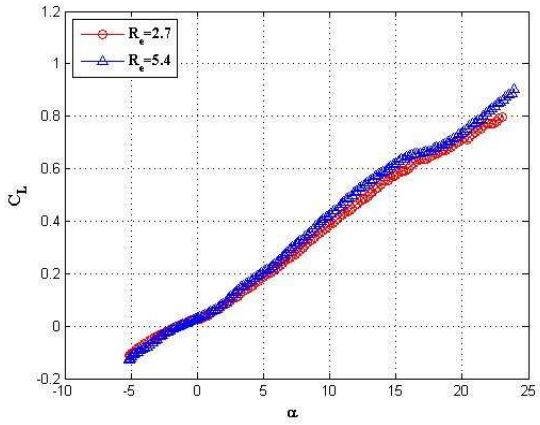

Figure 3. R_e effect at M=0.3 on R_{le}=0.0mm

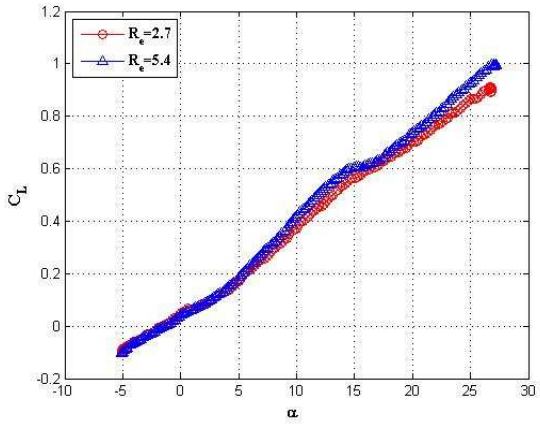

Figure 4. R_e effect at M=0.3 on R_{le}=0.625mm

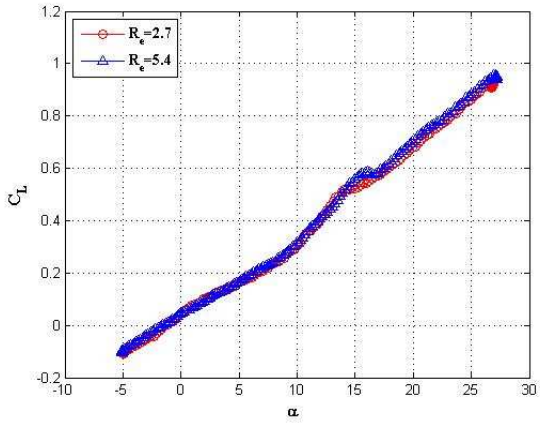

Figure 5. R_e effect at M=0.3 on R_{le}=1.25mm

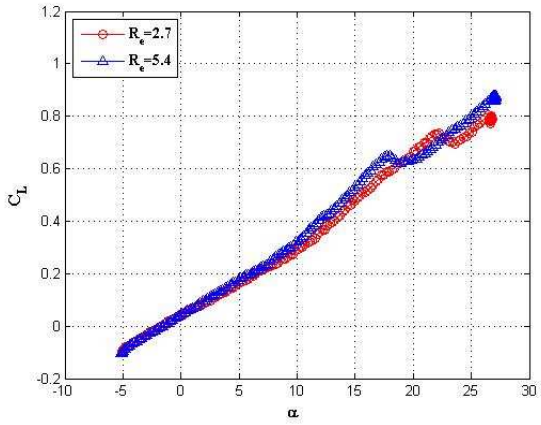

Figure 6. R_e effect at M=0.3 on R_{le}=2.5mm

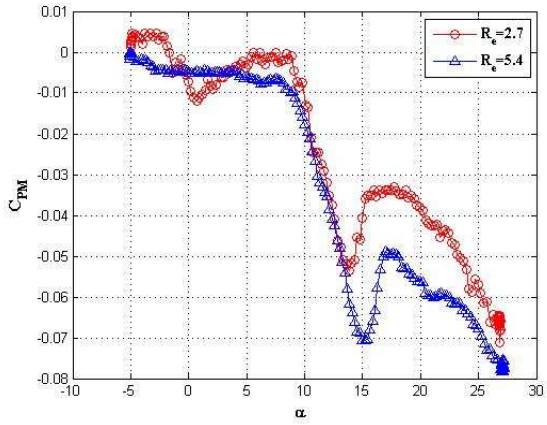

Figure 9. R_e effect at M=0.3 on R_{le}=1.25mm

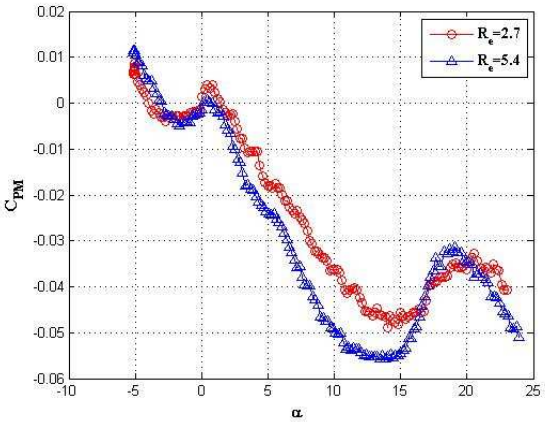

Figure 7. R_e effect at M=0.3 on R_{le}=0.0mm

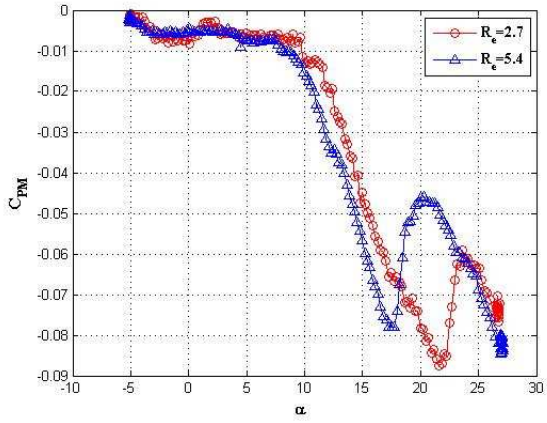

Figure 10. R_e effect at M=0.3 on R_{le}=1.25mm

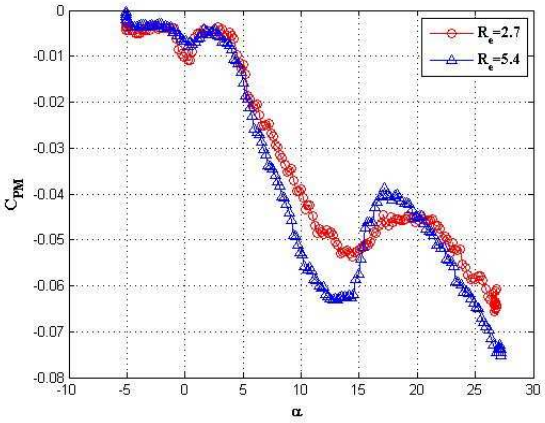

Figure 8. R_e effect at M=0.3 on R_{le}=0.625mm

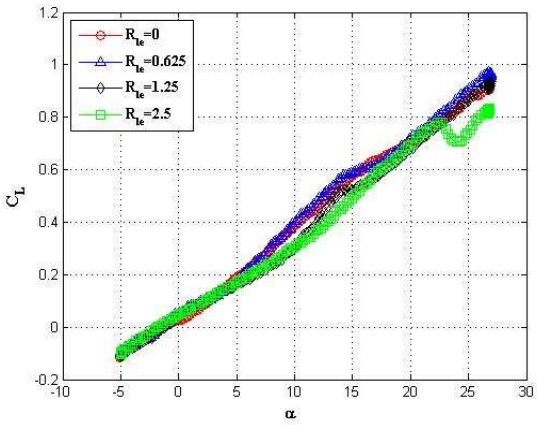

Figure 11. LE bluntness effect at M=0.3; R_e=2.7 million

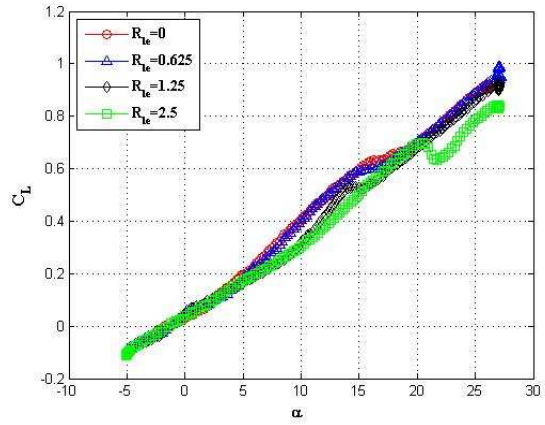

Figure 12. LE bluntness effect at M=0.4; R_e= 3.4 million

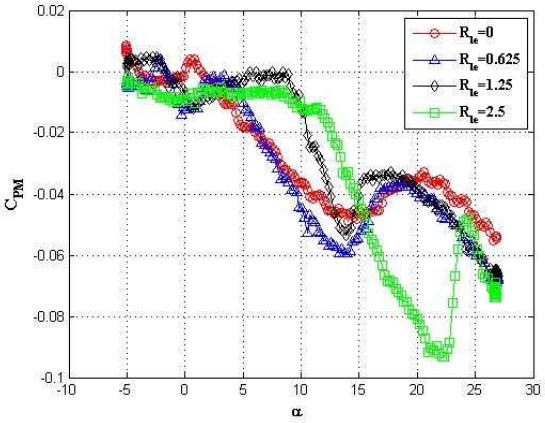

Figure 13. LE bluntness effect at M=0.3; R_e=2.7 million

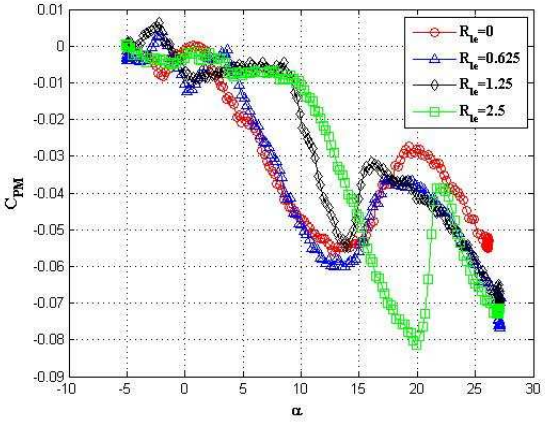

Figure 14. LE bluntness effect at M=0.4; R_e= 3.4 million

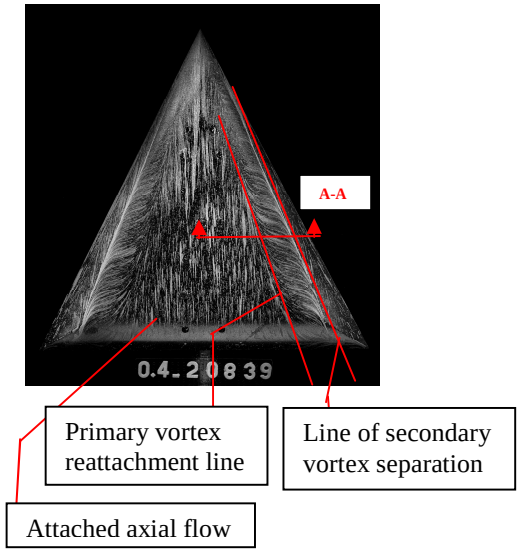

Figure 15. Oil flow at α =15° on R_{le}=0.0mm (sharp)

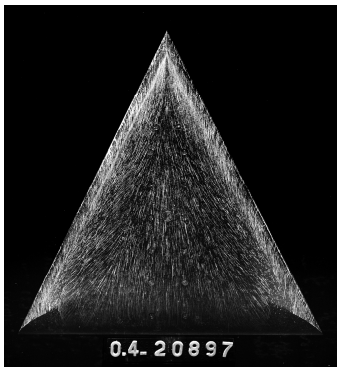

Figure 16. Oil flow at α =15° on R_{le}=2.5mm (large)

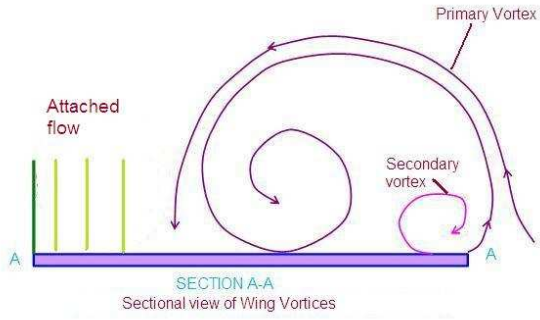

Figure 17. Sectional view of wing vortices for R_{le}=0.0mm at α =15°